AN EFFICIENT NUMERICAL RESOLUTION FOR MRI RICIAN DENOISING

A. Martín[1], J. F. Garamendi [2] and E. Schiavi[3]

[1]*Fundación CIEN-Fundación Reina Sofía, Madrid, Spain*
[2]*Departamento de Tecnología Electrónica, Universidad Rey Juan Carlos, Madrid, Spain*
[3]*Departamento de Matemática Aplicada, Universidad Rey Juan Carlos, Madrid, Spain*

Keywords: MRI Rician Denoising, Total Variation, Numerical Resolution, ROF Model.

Abstract: We consider a variational Rician denoising model for Magnetic Resonance Images (MRI) that we solve by a semi-implicit numerical scheme, which leads to the resolution of a sequence of Rudin, Osher and Fatemi (ROF) models. This allows to implement efficient numerical gradient descent schemes based on the dual formulation of the ROF model which are compared with a direct semi-implicit approach for the primal problem recently proposed for model validation. In this new framework the total variation operator is exactly solved as opposed to the approximating problems which must be considered when the primal problem is dealt with. The comparison among the above methods is performed using synthetic and real MR brain images and the results show the effectiveness of the new method in both, the accuracy and the speeding up of the algorithm.

1 INTRODUCTION

Modelling MRI denoising, a fundamental step in medical image processing, leads naturally to the assumption that MR magnitud images are corrupted by Rician noise which is a signal dependent noise (see (Henkelman, 1985), (Gudbjartsson and Patz, 1995) and (Sijbers et al., 1998)). In fact this noise is originated in the computation of the magnitude image from the real and imaginary images, that are obtained from the inverse Fourier Transform applied to the original raw data. This process involves a non-linear operation which maps the original Gaussian distribution of the noise to a Rician distribution, (Lysaker et al., 2003).

Nevertheless it is usually argued that this bias do not affect seriously the processing and subsequent analysis of MR images and a gaussian noise, identically distributed and not signal dependent, is modeled. To go beyond the unlikely assumption of gaussian noise, we consider, in a variational framework, a denoising model for MR Rician noise contaminated images recently considered in (Martín et al., 2011), which combines the Total Variation semi-norm with a data fitting term (see also (Basu et al., 2006) for an application to DT-MRI data denoising where low SNR Diffusion Weighted Images (DWI) are acquired). When the resulting functional is considered

for minimization, the variational approach leads to the resolution of a nonlinear degenerate PDE elliptic equation as the Euler Lagrange equation for optimization. This has a number of theoretical problems when the Total Variation operator is considered as a smoother, because the energy functional is not differentiable at the origin (i.e. $\nabla u = \bar{0}$) and regular, approximating problems must be solved. In turn this approach cause a over-smoothing effect in the numerical solutions of the model and accuracy in fine scale details is lost because the edges diffuse. A direct gradient descent method has been used in (Martín et al., 2011) in order to validate the model assumption of rician noise but the method is found to be inherently slow because a stabilization at the steady state is needed. Also, that scheme is finally explicit and very small time steps have to be used to avoid numerical oscillations.

Our aim is to present a new framework to solve numerically and efficiently the gradient descent scheme (gradient flow) associated to the Rician energy minimization problem introducing a new semi-implicit formulation. Using a simple Euler discretization of the time derivative, stationary problems of the Rudin, Osher and Fatemi (ROF) type (Rudin et al., 1992) are deduced. This allows to use the well known dual formulation of the ROF model proposed in (Chambolle, 2004) for a speed up of the computa-

tions. As a by-product of this approach the exact Total Variation operator can be computed and this provides accuracy to the solution in so far truly (discontinuos) bounded variation solutions are numerically approximated.

This paper is organized as follows: in section 2 and 3 we present the model equation and the numerical scheme recently proposed in (Martín et al., 2011). In section 4 we propose a new framework which leads to a more efficient and accurate numerical scheme. The proposed method is tested in section 5, where we consider synthetic MR brain images to compare it with the method of (Martín et al., 2011) and some preliminary results of applying this algorithm to real Diffusion Weighted Magnetic Resonance Images (DW-MRI) are shown in subsection 5. Finally in section 6 we present our conclusions.

2 MODEL EQUATIONS

Let Ω be a bounded open subset of $\mathbb{R}^d$, $d = 2, 3$ defining the image domain and let $f : \Omega \to \mathbb{R}$ be a given noisy image representing the data, with $f \in L^\infty(\Omega) \cap [0, 1]$ (otherwise we normalize). Let $BV(\Omega)$ be the space of functions with bounded variation in Ω equipped with the seminorm $|u|_{BV}$ defined as

$$|u|_{BV} = \sup \left\{ \int_\Omega u(x) \operatorname{div} \bar{\xi}(x) \, dx : \right.$$
$$\left. \bar{\xi} \in C_c^1(\Omega, \mathbb{R}^d), |\bar{\xi}(x)|_\infty \leq 1, x \in \Omega \right\} \quad (1)$$

where $|\cdot|_\infty$ denotes the l_∞ norm in $\mathbb{R}^d$, $|\bar{\xi}|_\infty = \max_{1 \leq i \leq d} |\xi_i|$ (details on this space and the related geometric measure theory can be found in (Ambrosio et al., 2000)). Following a Bayesian modelling approach we consider the minimization problem

$$\min_{u \in BV(\Omega)} \left\{ J(u) + \lambda H(u, f) \right\} \quad (2)$$

where $J(u)$ is the convex nonnegative total variation regularization functional

$$J(u) = |u|_{BV} = |Du|(\Omega) \quad (3)$$

being $|Du|(\Omega)$ the Total variation of u with Du its generalized gradient (a vector bounded Radon measure). When $u \in W^{1,1}(\Omega)$ we have $|Du|(\Omega) = \int_\Omega |\nabla u| dx$. The λ parameter in (2) is a scale parameter tuning the model.

The data term $H(u, f)$ is a fitting functional which is nonnegative with respect to u for fixed f. To model rician noise the form of $H(u, f)$ has been deduced in (Basu et al., 2006) in the context of weighed diffusion tensor MR images. The Rician likelihood term is of the form:

$$H(u, f) =$$
$$\int_\Omega \left(\left(\frac{u^2 + f^2}{2\sigma^2} \right) - \log I_0 \left(\frac{uf}{\sigma^2} \right) - \log \left(\frac{f}{\sigma^2} \right) \right) dx \quad (4)$$

where σ is the standard deviation of the rician noise of the data and I_0 is the modified zeroth-order Bessel function of the first kind. Notice that the constant terms $(1/2\sigma^2)\|f\|_2^2$ and $\int_\Omega \log(f/\sigma^2)$ appearing in (4) do not affect the minimization problem. Dropping these terms (which do not allows to define the energy $H(u, 0)$ corresponding to a black image $f \equiv 0$) we have:

$$H(u, f) = \frac{1}{2\sigma^2} \int_\Omega u^2 dx - \int_\Omega \log I_0 \left(\frac{uf}{\sigma^2} \right) dx \quad (5)$$

with $H(u, 0) = (1/2\sigma^2)\|u\|_2^2$ and $H(0, f) = 0$ for any given $f \geq 0$. Using (2), (3) and (5) the minimization problem is formulated as:

Fixed λ and σ and given a noisy image $f \in L^\infty(\Omega) \cap [0, 1]$ recover $u \in BV(\Omega) \cap L^\infty(\Omega) \cap [0, 1]$ minimizing the energy:

$$J(u) + \lambda H(u, f) = |Du|(\Omega) +$$
$$+ \frac{\lambda}{2\sigma^2} \int_\Omega u^2 dx - \lambda \int_\Omega \log I_0 \left(\frac{uf}{\sigma^2} \right) dx \quad (6)$$

Due to the fact that the functional in (3) (hence in (6)) is not differentiable at the origin we introduce the subdifferential of $J(u)$ at a point u by

$$\partial J(u) = \{ p \in BV(\Omega)^* | J(v) \geq J(u) + < p, v - u > \}$$

for all $v \in BV(\Omega)$, to give a (weak and multivalued) meaning to the Euler-Lagrange equation associated to the minimization problem (6). In fact the first order optimality condition reads

$$\partial J(u) + \lambda \partial_u H(u, f) \ni 0 \quad (7)$$

with (Gâteaux) differential

$$\partial_u H(u, f) = \left(\frac{u}{\sigma^2} \right) - \left[I_1 \left(\frac{uf}{\sigma^2} \right) / I_0 \left(\frac{uf}{\sigma^2} \right) \right] \left(\frac{f}{\sigma^2} \right)$$

where I_1 is the modified first-order Bessel function of the first kind and verifies ((Lassey, 1982)) $0 \leq I_1(\xi) / I_0(\xi) < 1, \forall \xi > 0$. This model, first proposed in (Martín et al., 2011), differs from (Basu et al., 2006) because of the geometric prior (the TV-based regularization term) which substitutes their Gibb's prior model based on the Perona and Malik energy functional (Perona and Malik, 1990) . Also it differs from the classical gaussian noise model because of the nonlinear dependence of the solution of the ratio I_1/I_0.

3 THE PRIMAL DESCENT GRADIENT NUMERICAL SCHEME

A number of mathematical difficulties is associated with the multivalued formulation (7) and a regularization of the diffusion term $\text{div}\,(\nabla u/|\nabla u|)$ in form $\text{div}\,(\nabla u/|\nabla u|_\varepsilon)$, with $|\nabla u|_\varepsilon = \sqrt{|\nabla u|^2 + \varepsilon^2}$ and $0 < \varepsilon \ll 1$ is implemented to avoid degeneration of the equation where $\nabla u = \bar{0}$. Using this approximation it is possible to give a (weak) meaning to the following formulation:

Fixed λ, σ and (small) ε and given $f \in L^\infty(\Omega) \cap [0,1]$ find $u_\varepsilon \in W^{1,1}(\Omega) \cap [0,1]$ solving

$$-\text{div}\left(\frac{\nabla u_\varepsilon}{|\nabla u_\varepsilon|_\varepsilon}\right) + \frac{\lambda}{\sigma^2}\left[u_\varepsilon - r_\varepsilon(u_\varepsilon, f)f\right] = 0 \quad (8)$$

complemented with Neumann homogeneous boundary cond itions $\partial u_\varepsilon / \partial n = 0$ and where, for notational simplicity, we introduced the nonlinear function $r_\varepsilon(u_\varepsilon, f) = I_1(u_\varepsilon f/\sigma^2)/I_0(u_\varepsilon f/\sigma^2)$.

This is a nonlinear (in fact quasilinear) elliptic problem that we solve with a gradient descent scheme until stabilization (when $t \to +\infty$) of the evolutionaty solution to steady state, i.e. a solution of the elliptic problem (8) which is a minimum of the energy

$$J_\varepsilon(u_\varepsilon) + \lambda H(u_\varepsilon, f) = \int_\Omega \sqrt{|\nabla u_\varepsilon|^2 + \varepsilon^2}\,dx +$$

$$+ \frac{\lambda}{2\sigma^2}\int_\Omega u^2 dx - \lambda \int_\Omega \log I_0\left(\frac{uf}{\sigma^2}\right)dx \quad (9)$$

When $\varepsilon \to 0$ we have $u_\varepsilon \to u$, $J_\varepsilon(u_\varepsilon) \to J(u)$ and the energies in (6) and (9) coincide.

This approach amounts to solve the associated nonlinear parabolic problem:

$$\frac{\partial u_\varepsilon}{\partial t} = \text{div}\left(\frac{\nabla u_\varepsilon}{|\nabla u_\varepsilon|_\varepsilon}\right) - \frac{\lambda}{\sigma^2}\left[u_\varepsilon - r_\varepsilon(u_\varepsilon, f)f\right] \quad (10)$$

complemented with Neumann homogeneous boundary conditions $\partial u_\varepsilon / \partial n = 0$ and initial condition $u_\varepsilon(0,x) = u_0^\varepsilon(x)$ whose (weak) solution stabilizes (when $t \to +\infty$) to the steady state of (8), i.e. a minimum of (9) which approximates, for ε sufficiently small, a minimum of the energy functional (6). Following (Martín et al., 2011) and using forward finite difference for the temporal derivative it is straightforward to define a semi-implicit iterative scheme which simplifies to the explicit one:

$$\left(1 + \Delta t\frac{\lambda}{\sigma^2}\right)u_\varepsilon^{n+1} =$$

$$= u_\varepsilon^n + \Delta t\left(\text{div}\left(\frac{\nabla u_\varepsilon^n}{|\nabla u_\varepsilon^n|_\varepsilon}\right) + \frac{\lambda}{\sigma^2}r(u_\varepsilon^n, f)f\right) \quad (11)$$

where Δt is the time step and spatial discretization for the approximated TV-term is performed as in (Nikolova et al., 2006) .

4 A SEMI-IMPLICIT FORMULATION

In the previous section we considered the approximated Euler-Lagrange equation (8) associated to the minimization of the energy (6). This is a modelling approximation and we can get rid of it. In fact, considering the original Euler-Lagrange equation associated to the energy (6) we have (with abuse of notation for the diffusive term)

$$-\text{div}\left(\frac{\nabla u}{|\nabla u|}\right) + \frac{\lambda}{\sigma^2}\left[u - r(u,f)f\right] = 0 \quad (12)$$

with $r(u,f) = I_1(uf/\sigma^2)/I_0(uf/\sigma^2)$. A rigorous treatment of equation (12) should follow the multivalued formalism of (7).

Using again a gradient descent scheme we have to solve the parabolic problem:

$$\frac{\partial u}{\partial t} = \text{div}\left(\frac{\nabla u}{|\nabla u|}\right) - \frac{\lambda}{\sigma^2}\left[u - r(u,f)f\right] \quad (13)$$

together with Neumann homogeneous boundary conditions $\partial u/\partial n = 0$ and initial condition $u(0,x) = u_0(x)$. For comparison purposes we used $u_0(x) = u_0^\varepsilon(x)$ in all numerical tests.

Using forward finite difference for the temporal derivative in (13) and a semi-implicit scheme where only the term depending on the ratio of the Bessel's functions is delayed, results in the numerical scheme:

$$\left(1 + \Delta t\frac{\lambda}{\sigma^2}\right)u^{n+1} =$$

$$= u^n + \Delta t\left(\text{div}\left(\frac{\nabla u^{n+1}}{|\nabla u^{n+1}|}\right) + \frac{\lambda}{\sigma^2}r(u^n, f)f\right) \quad (14)$$

where the diffusive term is (formaly) exact and implicitly considered (compare with (11)). Defyining $\alpha = (\lambda\Delta t + \sigma^2)/(\lambda\Delta t)$ and

$$\alpha\hat{f}_n = \left(\frac{\sigma^2}{\lambda\Delta t}\right)u^n + r(u^n, f)f$$

we can write:

$$-\text{div}\left(\frac{\nabla u^{n+1}}{|\nabla u^{n+1}|}\right) + \left(\frac{\alpha\lambda}{\sigma^2}\right)\left[u^{n+1} - \hat{f}_n\right] = 0 \quad (15)$$

17

(a) Original phantom   (b) Noisy for $\sigma = 0.025$ (c) Noisy for $\sigma = 0.05$ (d) Noisy for $\sigma = 0.1$

(e) Original phantom   (f) Denoised for $\sigma = 0.025$, $\lambda = 0.025$ (g) Denoised for $\sigma = 0.05$, $\lambda = 0.075$ (h) Denoised for $\sigma = 0.1$, $\lambda = 0.125$
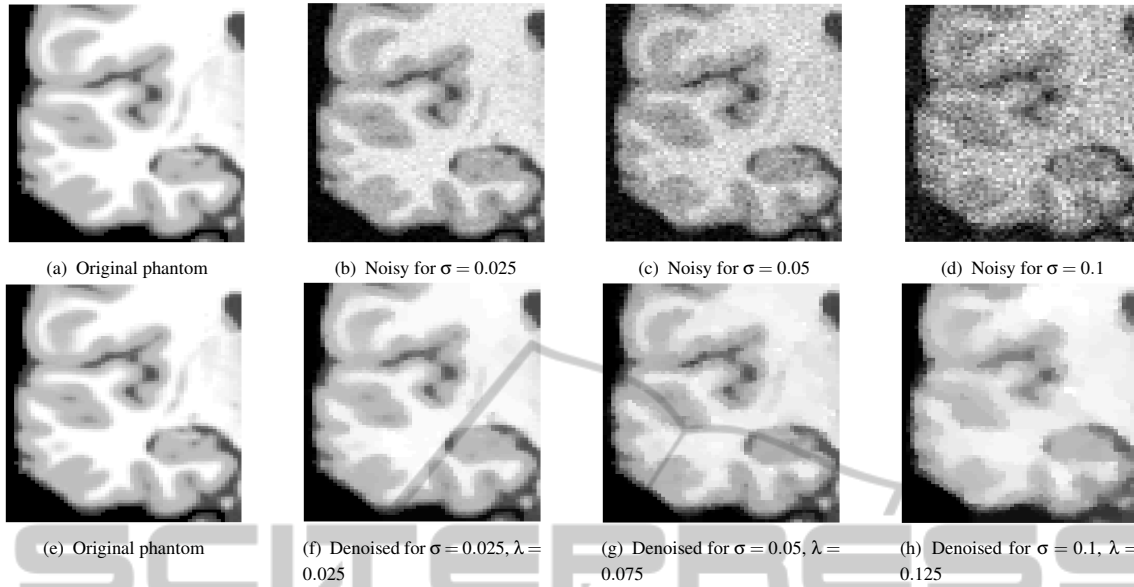
Figure 1: The original free noise phantom is shown in images a) and e). In b), c) and d) the contaminated phantoms for $\sigma = 0.025$, 0.05 and 0.1 respectively. Below, their respective denoised images e), f) and g) for $\lambda = 0.025$, 0.075 and 0.125.

which is the Euler-Lagrange equation of the ROF energy functional ((Rudin et al., 1992)):

$$E(u) = |Du|(\Omega) + \left(\frac{1}{2\beta}\right) \int_\Omega (u - g)^2 dx \qquad (16)$$

for $\beta = \sigma^2/(\alpha\lambda)$ and $g = \hat{f}_n$, for any positive integer $n > 0$, with (artificial) time $t_n = n\Delta t$. Hence, at each gradient descent step Δt, we can solve a ROF problem associated to the minimization of the energy (16) in the space $BV(\Omega) \cap [0, 1]$. This problem is mathematically well-posed and it can be numerically solved by very efficient methods, when formulated using well known duality arguments (see (Chambolle, 2004) for more details).

5 RESULTS AND DISCUSSION

The theoretical result presented in the previous section have to be numerically confirmed in order to asses the well behaviour of the method and also the advantages it presents when it is compared to the original regularized method which computes the approximating u_ε solution. In order to assess the performance of our algorithm we tested it with synthetic and real brain images. The obtained results are presented and discussed below.

Synthetic Brain Images
The synthetic brain images we used for our study were obtained from the BrainWeb Simulated Brain

Database[1] at the Montreal Neurological Institute (Aubert-Broche et al., 2006) . The original phantoms were contaminated artificially with Rician noise considering the data as a complex image with zero imaginary part and adding random gaussian perturbations to both the real and imaginary part, before computing the magnitude image. This process allows to control the amount and distribution of the Rician noise so providing a gold standard for our study. For this we used different values of the σ parameter which represents the variance of the noise ($\sigma = 0.025$, $\sigma = 0.05$ and $\sigma = 0.1$) and different values of the λ parameter ($\lambda = 0.05$, $\lambda = 0.1$ and $\lambda = 0.125$). Notice that, fixed σ (which can be estimated for real images) the λ parameter is the only one we have to choose for regularization (as in the gaussian case).

We can observe in Figure 1 the performance of the denoising method based on the semi-implicit formulation for $\lambda = 0.05$, $\lambda = 0.1$ and $\lambda = 0.125$. This implicit method solves exactly the total variation operator in (6) due to its dual formulation and not its approximate form as the explicit method which solves the primal formulation, so the solution obtained should be close to the ideal minimum of (6). This behaviour can be in fact observed in Figure 2, where using the same values for the algorithms ($\Delta t = 10^{-3}$ and $\lambda = 0.1$) the proposed method reach a solution whose energy is smaller than the obtained by the solution of the first method. This difference caused by the fact that now we are using the true Total Vari-

---

[1] available at http://www.bic.mni.mcgill.ca/brainweb
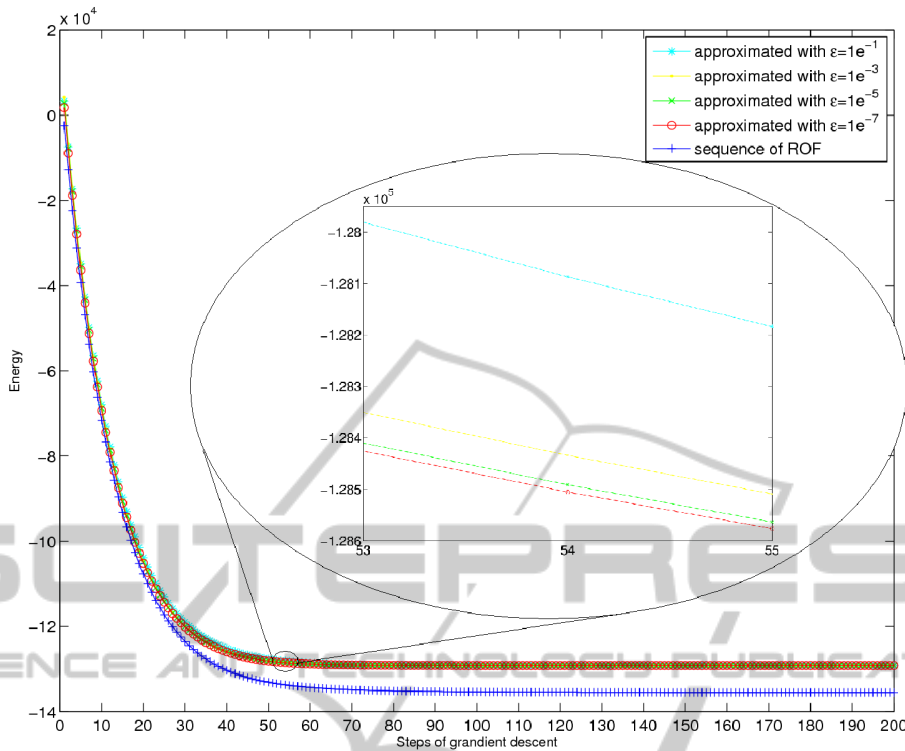
Figure 2: Energy in functional 6 of the solution obtained at each step of the gradient descent by the approximated method for $\lambda = 0.1$, $\sigma = 0.05$, $dt = 0.001$ and different values of $\varepsilon = 10^{-1}, 10^{-3}, 10^{-5}, 10^{-7}$, and by the new method for $\lambda = 0.1$, $\sigma = 0.05$, $dt = 0.001$.

ation can be also observed in the images of the absolute difference between the original (free of noise) image and the solutions found by the two methods. We can see how the image difference corresponding to the solution of the approximated method (Figure 3 a) presents more structural details than the image corresponding to the implicit method (Figure 3 b), which confirms that this last method recovers more structural details, that are eventually lost by the explicit method because of the ε approximation.

The other important characteristic of this new formulation is that the diffusion term is implicitly considered and this provides numerical stability which in turn allows to increase the value of Δt compared to those used in the explicit method, so less iterations of the algorithm are necessary for time stabilization. In fact if we increase the value of Δt to the value $\Delta t = 10^{-1}$ the explicit method becomes unstable and it begins to oscillate without reaching the minimum of the energy we obtained with $\Delta t = 10^{-3}$. Also the implicit method takes less iterations to reach the same minimum. The performance of the two algorithms for $\Delta t = 10^{-1}$ can be observed in Figure 4 where the energy computed along the iterates of the implicit method is clearly less than the same energy

calculated along the approximated iterates.

This behaviour is crucial for the selection of the algorithm in so far even if the new method has more computational cost per iteration (because we solve a ROF problem at each iteration), we can increase the value of Δt in order to reach the solution in less iterations than the first method, finding a best solution for our problem (in the sense of figure 4) and spending less time of computation. Finally, in the last figure(figure 5) we show that this framework is robust in the sense that the same solution is obtained when completely different initial condition are used for initialization in the gradient flow schemes we considered. This is suggestive of uniqueness for the non trivial solution of the corresponding elliptic problems.

Real Brain Images
Apart from the modelling exercise and the implementation details of the algorithm presented above, our main interest relies in the application of the proposed algorithm to real brain images. In the following we present some preliminary results we are obtaining for Diffusion Weighted Magnetic Resonance Images (DW-MRI) denoising. The DW-MR images are acquired and used for Diffusion Tensor Image (DTI) re-

(a) Existing method   (b) Proposed method
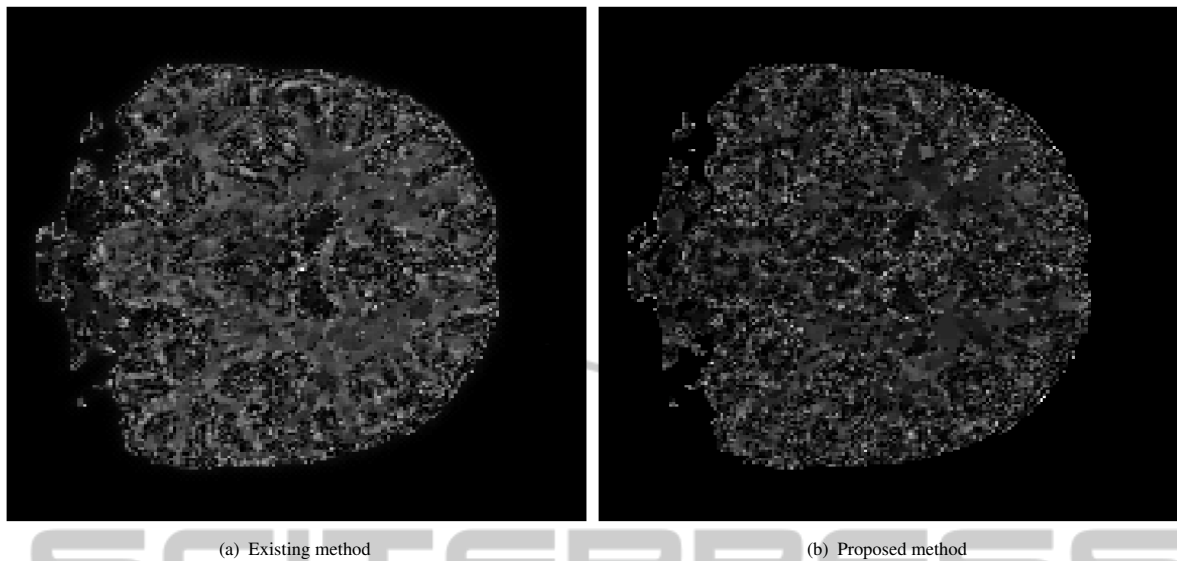
Figure 3: Absolute difference between the original image and the solution of the existing method and the proposed method for the values $\lambda = 0.1$, $\sigma = 0.05$, $dt = 0.001$ in both methods and $\varepsilon = 10^{-7}$ for the approximated method.
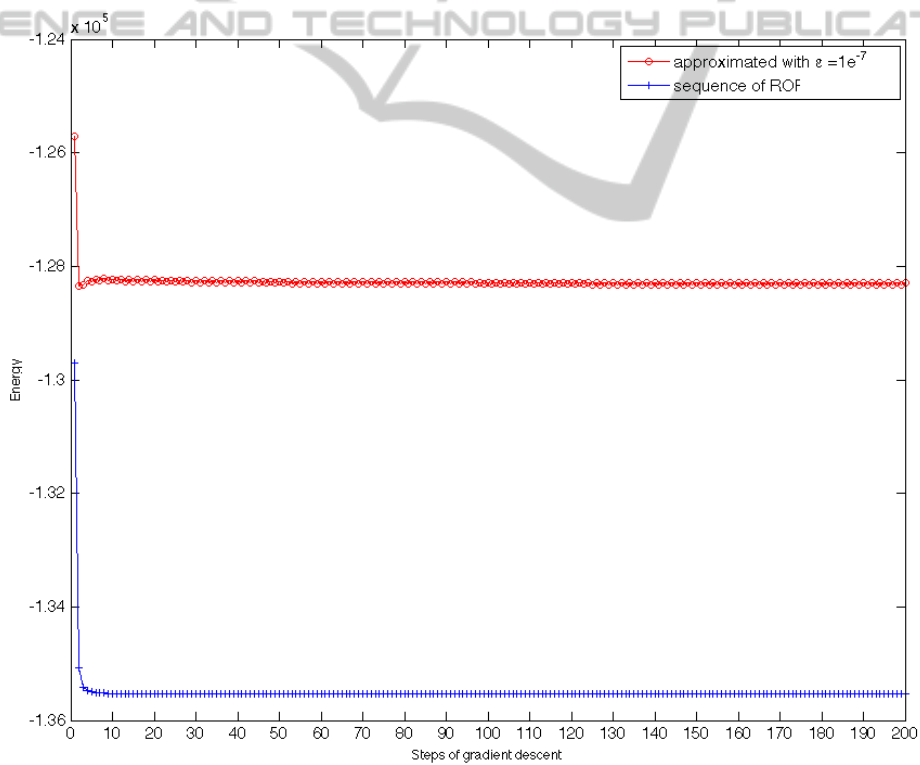
Figure 4: Energy in functional 6 of the solution obtained at each step of the gradient descent by the approximated method for $\varepsilon = 10^{-7}$, $\lambda = 0.1$, $\sigma = 0.05$, $dt = 0.1$ and by the new method for $\lambda = 0.1$, $\sigma = 0.05$, $dt = 0.1$.

construction, and the importance of the denoising step is crucial in DW-MRI analysis because their characteristic very low SNR (Basu et al., 2006). Diffusion Tensor Imaging is a MRI technique that can measure the water diffusion which is restricted by the surrounding structure, and this allows to infer the macroscopic axonal organization in nervous system tissues. We show the results of the DTI reconstruction for
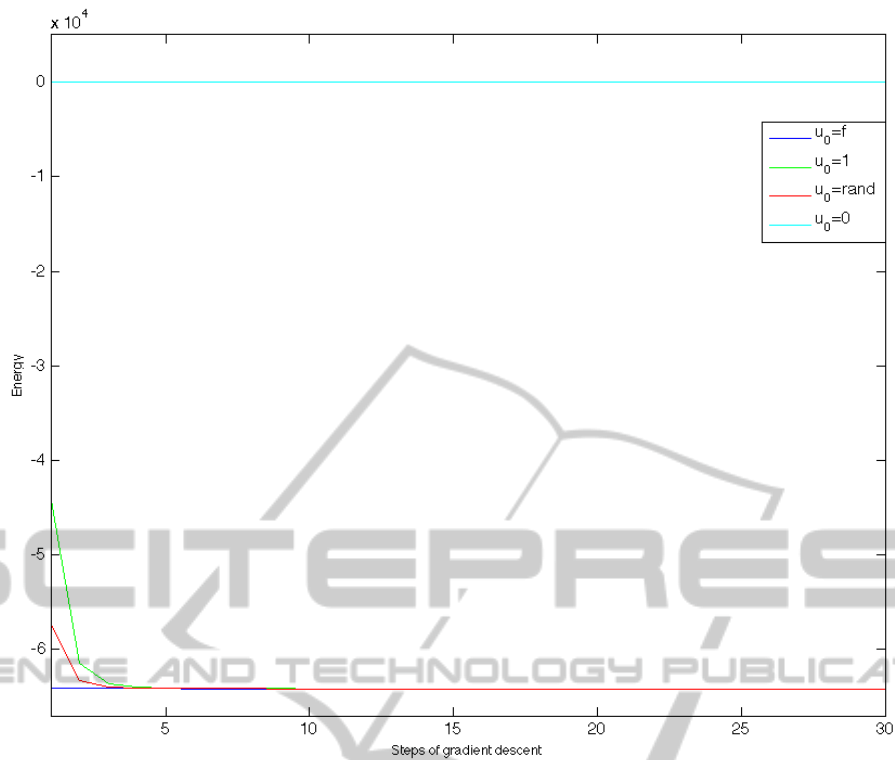
Figure 5: Energy in functional 6 of the solution obtained at each step of the gradient descent by the new method for $\lambda = 0.05$, $\sigma = 0.05$, $dt = 0.1$ and different initial data u_0: black image ($u_0 \equiv \bar{0}$), white image ($u_0 \equiv \bar{1}$), the noisy image ($u_0 \equiv f$) and a random image ($u_0 \equiv rand$).

(a) Original   (b) Denoised with $\lambda = \sigma/2$ (c) Denoised with $\lambda = \sigma/4$
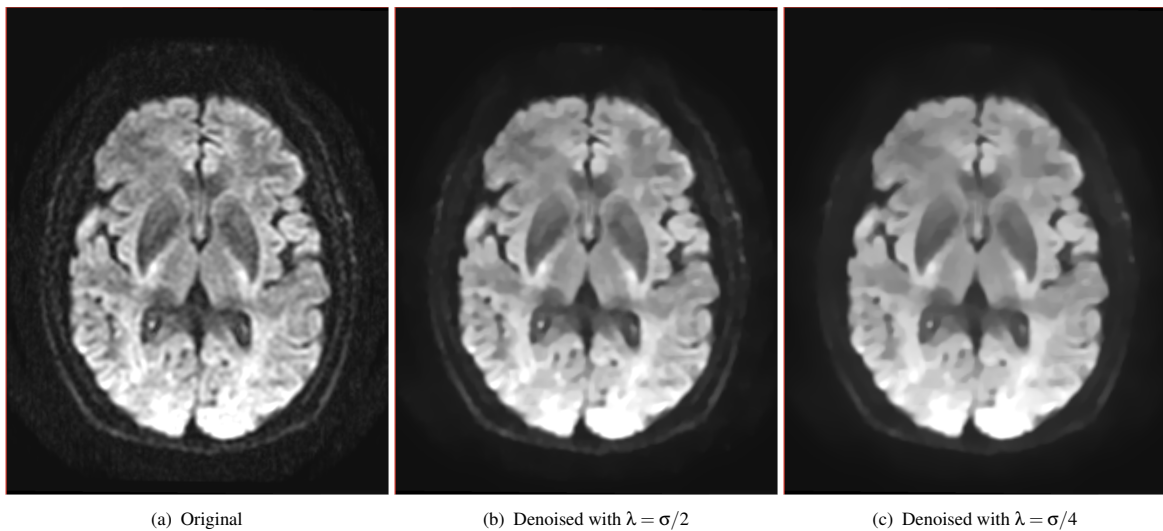
Figure 6: A slice of the original Diffusion Weighted Image corresponding to the (1, 0, 0) gradient direction and the corresponding denoised images.

the original DW-MRI data and the correspondent denoised data with different values of the parameter λ.

For this preliminary study we have used a DW-MR brain volume provided by Fundación CIEN-Fundación Reina Sofía which was acquired with a 3 Tesla General Electric scanner equipped with an 8-channel coil. The DW images have been obtained with a single-shot spin-eco EPI sequence (FOV=24cm, TR=9100, TE=88.9, slice thickness=3mm, spacing=0.3, matrix size=128x128,

(a) From original DWI data   (b) From denoised DWI data with $\lambda = \sigma/2$ (c) From denoised DWI data with $\lambda = \sigma/4$
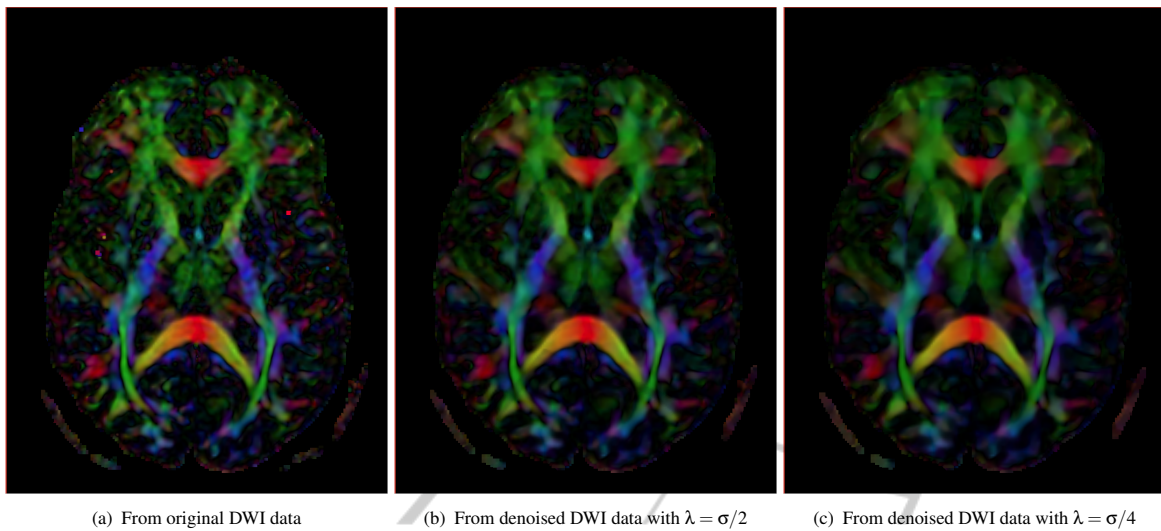
Figure 7: A slice of the colormap orientation (of the main eigenvector) of the DTI data. red means right-left direction, green anterior-posterior and blue inferior-superior. Fibers with an oblique angle have a color that is a mixture of the principal colors and black color is used for the isotropic regions as the cerebrospinal fluid.

(a) From original DWI data   (b) From denoised DWI data with $\lambda = \sigma/2$ (c) From denoised DWI data with $\lambda = \sigma/4$
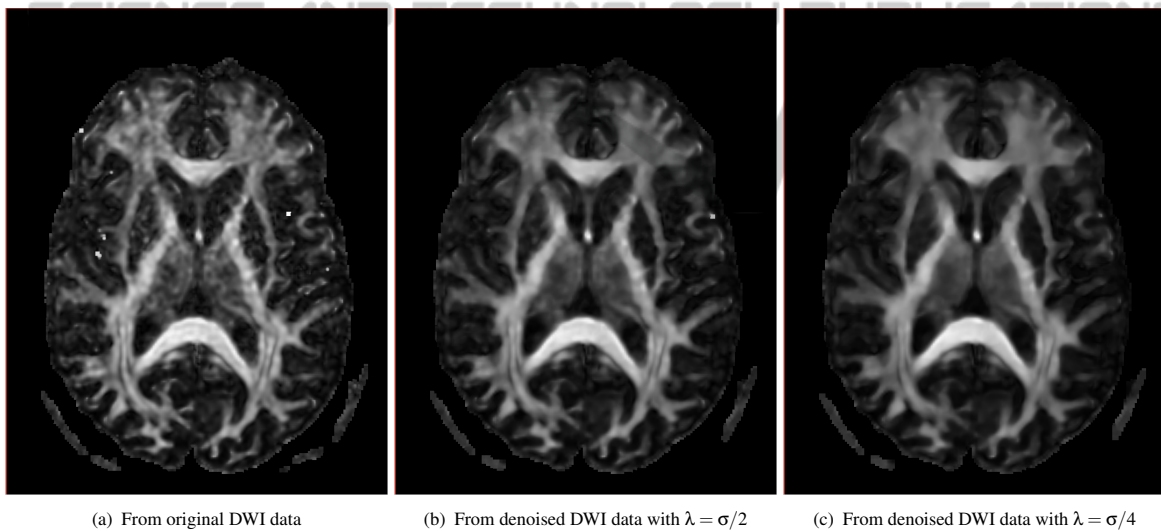
Figure 8: A slice of the Fractional Anisotropy estimated from the Tensor Image. Dark colour corresponds to values near zero (isotropic regions) and bright color corresponds to values near one (anisotropic regions).

NEX=2). The DW-MRI data consists on a volume obtained with b=0/mm^2 and 15 volumes with b=1000s/mm^2 corresponding with the gradient directions specified in (DK Jones, 1999). These DW-MR images, which represent diffusion measurements along multiples directions, are denoised with the proposed method previously to the Diffusion Tensorial Image reconstruction, which was done with the 3d Slicer tools[2].

In Figure 6(a) we show a slice of the original DWI

data corresponding to the (1, 0, 0) gradient direction where the affecting noise is clearly visible. The complete DW-MRI data volume is denoised using the proposed method where the Rician noise magnitude (σ) has been estimated for each gradient direction following (Sijbers et al., 1998), while we have used two different values of λ for the denoising, $\lambda = \sigma/2$ and $\lambda = \sigma/4$. The two slices resulting from the denoising process are shown in Figures 6(b) and 6(c). It can be observed that smaller values of λ provide stronger diffusion (which is coherent with the model formulation in 6) and how in the two denoised images the noise

[2]Free available in http://www.slicer.org/

has been removed but the details and the edges have been fully preserved, as we should expect when the exact TV model is solved.

The effect of this denoising process over the reconstructed tensor and their derived scalar measurements (obtained with the 3d Slicer tools) is presented in Figures 7 and 8. Figure 7 shows a color-coded orientation map created from DTI data. In this image, the principal colors (red, green, and blue) represent fibers running along the spatial orientations (x, y, z). Results in 7 shows that the structures are better defined if the DW-MRI volume is denoised previously. As evidenced by Figure 8 this effect is yet more visible in the measurements like the Fractional Anisotropy where the structures and details are clearly enhanced. When we use a lower value for λ (Figures 7(c) and 8(c)) we obtain smoother tensorial images but some details can be better distinguished when the value of λ is higher (Figures 7(b) and 8(b)).

6 CONCLUSIONS

In this notes we address the problem of the numerical computation of the solution of the variational formulation of the Rician denoising model proposed in (Martín et al., 2011). We deduce a semi-implicit formulation for the gradient flow which leads to the resolution of ROF like-problems at each step of the time discretization. This is accomplished efficiently using a gradient descent for the dual variable associated to the primal ROF model. While our study is preliminary it indicates how to obtain fast numerical solutions for Rician denoising. This is specially interesting when Diffusion Wheighted Images (DWI) are considered for Diffusion Tensor Images reconstruction whereas they have poor resolution and low SNR which makes Rician denoising necessary.

Challenging mathematical issues arise about the existence, uniqueness and convergence, when $\varepsilon \to 0$, of weak bounded variation solutions of the quasilinear elliptic equations considered in this paper (i.e. (8) and (12)) and the gradient flow analysis of their parabolic counterpart ((10) and (13)) when $t \to +\infty$. A rigorous justification of the above arguments is desired. Nevertheless this approach is the mostly used regularization technique to approximate and compute the minimizer of the total variation energy and its variants (see (Casas et al., 1998)).

The semi-implicit method we propose is well founded mathematically when the time-discretized problems are dealt with and it represents a feasible alternative to gaussian denoising for low SNR MR images. Further study is undoubtedly necessary in order

to make automatic the choice of the parameters in real medical images. Other possibilities, such as Inverse scaling, which makes the parameter estimation less crucial and provide contrast enhanced images shall also be explored.

ACKNOWLEDGEMENTS

REFERENCES

Ambrosio, L., Fusco, N., and Pallara, D. (2000). *Functions of Bounded Variation and free discontinuity problems*. The Clarendon Press, Oxford University.

Aubert-Broche, B., Griffin, M., Pike, G., Evans, A., and Collins, D. (2006). Twenty new digital brain phantoms for creation of validation image data bases. In *IEEE transactions on Medical Imaging*, volume 25, pages 1410–1416.

Basu, S., Fletcher, T., and Whitaker, R. (2006). Rician noise removal in diffusion tensor mri. *Medical Image Computing and Computer-Assisted Intervention*, 9(Pt 1):117–125.

Casas, E., Kunisch, K., and Pola, C. (1998). Some applications of bv functions in optimal control and calculus of variations. In *ESAIM: Proceedings. Control and partial differential equations*, volume 4, pages 83–96.

Chambolle, A. (2004). An algorithm for total variation minimization and applications. *Journal Mathematical Imaging and Vision*, 20:89–97.

DK Jones, MA Horsfield, A. S. (1999). Optimal strategies for measuring diffusion in anisotropic systems by magnetic resonance imaging. *Journal of Magnetic Resonance in Medicine*, 42 (3):515–525.

Gudbjartsson, H. and Patz, S. (1995). The rician distribution of noisy mri data. *Magnetic Resonance in Medicine*, 34(6):910–914.

Henkelman, R. M. (1985). Measurement of signal intensities in the presence of noise in mr images. *Medical Physics*, 12(2):232–233.

Lassey, K. R. (1982). On the computation of certain integrals containing the modified bessel function $i_0(\xi)$. *Mathematics of Computation*, 39.

Lysaker, M., Lundervold, A., and cheng Tai, X. (2003). Noise removal using fourth-order partial differential equations with applications to medical magnetic resonance images in space and time. *IEEE Trans. Imag. Proc*, 12:1579–1590.

Martín, A., Garamendi, J., and Schiavi, E. (2011). Iterated rician denoising. In *IPCV'11 Proceedings*, Las Vegas, Nevada, USA. CSREA Press.

Nikolova, M., Esedoglu, S., and Chan, T. F. (2006). Algorithms for finding global minimizers of image segmentation and denoising models. *SIAM Journal of Applied Mathematics*, 66(5):1632–1648.

Perona, P. and Malik, J. (1990). Scale-space and edge detection using anisotropic diffusion. *Pattern Analysis and Machine Intelligence, IEEE Transactions on*, 12(7):629–639.

Rudin, L. I., Osher, S., and Fatemi, E. (1992). Nonlinear total variation based noise removal algorithms. *Physica D Nonlinear Phenomena*, 60:259–268.

Sijbers, J., Dekker, A. D., Audekerke, J. V., Verhoye, M., and Dyck, D. V. (1998). Estimation of the noise in magnitude mr images. *Magnetic Resonance Imaging*, 1(16):87–90.